

# Sound Transmission Through an Aeroelastic Plate into a Cavity

Kenneth D. Frampton\* and Robert L. Clark†

Duke University, Durham, North Carolina 27708-0302

Sound transmission through a convected fluid loaded plate, i.e., aeroelastic plate, backed by a reverberant acoustic cavity is investigated. The plate and cavity are modeled using Galerkin's method while the aerodynamic forces on the plate are approximated with a singular value decomposition method. Analytical results indicate that variations in the external flow velocity can significantly affect the sound transmission. The mechanism by which these effects occur is discussed. Also discussed is the importance of including the cavity coupling toward calculating the transmitted sound.

## Nomenclature

$a$	= plate length
$a_a$	= external speed of sound
$a_c$	= cavity speed of sound
$b$	= plate width
$C_{nm}$	= cavity/plate coupling coefficient
$D_{mn}$	= aerodynamic influence coefficient
$D_s$	= plate stiffness, $E_s I / (1 - \nu^2)$
$E^c$	= cavity potential energy
$H_{mn}(t)$	= aerodynamic influence function
$h_s$	= plate thickness
$I_{mn}(t)$	= aerodynamic influence function
$L_x, L_y, L_z$	= cavity dimensions
$M$	= Mach number
$M_n$	= modal mass
$m, n$	= modal indices
$\mathcal{P}(\omega)$	= cavity potential energy power spectrum
$\mathcal{P}_{q_n, q_n}(\omega)$	= disturbance generalized force power spectrum
$\bar{p}^a(x, y, t)$	= aerodynamic pressure
$p^c(x, y, t)$	= cavity pressure
$p^d(x, y, t)$	= disturbance pressure
$Q_n^a(t)$	= aerodynamic pressure generalized force
$Q_n^d(t)$	= disturbance pressure generalized force
$q_n(t)$	= plate generalized coordinate
$S_{mn}$	= aerodynamic influence coefficient
$t$	= time
$U_a$	= freestream velocity
$w(x, y, t)$	= panel displacement
$x, y, z$	= Cartesian coordinates
$\Gamma_m(x, y, z)$	= cavity modal expansion functions
$\Lambda_m$	= cavity modal volume
$\lambda$	= nondimensional dynamic pressure, $\rho_a U_a^2 a^3 / D_s$
$\rho_a$	= external fluid density
$\rho_c$	= cavity fluid density
$\rho_s$	= plate density
$\Phi^a(x, y, z, t)$	= external fluid velocity potential
$\Phi^c(x, y, z, t)$	= cavity fluid velocity potential
$\phi_m^c(t)$	= cavity generalized coordinate
$\Psi_n(x, y)$	= plate modal expansion functions
$\omega_m^*$	= cavity natural frequency
$\omega_h$	= plate natural frequency

## Introduction

THE reduction of sound transmission to aircraft interiors has been an important objective of aircraft manufacturers for many

years. The transmission of turbulent boundary-layer noise is of particular importance inasmuch as it is widely regarded as the dominant noise source (second, possibly, to engine noise). Therefore, a good understanding of the mechanisms and trends in noise transmission through elastic plates allows more effective application of noise control techniques, be they active or passive. A considerable amount of work has been done in the past toward understanding sound transmission and radiation from plates for these very reasons.<sup>1,2</sup> However, very few references are available that consider the effects of convected fluid loading on sound transmission through (or radiation from) plates.<sup>3-5</sup> Those that do consider it do not consider the implications of coupling with a reverberant acoustic environment. Therefore, the purpose of this work is to investigate the effects of sound transmission through a convected fluid loaded plate into a reverberant acoustic cavity.

A great deal of literature is available concerning the effects of convected fluid loading on plates, i.e., aeroelasticity. Early investigations by Dowell,<sup>6-8</sup> Dugundji,<sup>9</sup> and Hedgepeth,<sup>10</sup> among others, investigated the parametric stability boundaries of plates subjected to flow, i.e., panel flutter. Findings in these papers indicate that plate dynamics can be significantly affected by convected fluid loading.

Additionally, a considerable amount of work exists for investigations of cavity backed plates. Work by Dowell and Voss,<sup>11</sup> Fahy,<sup>12</sup> and Pretlove,<sup>13</sup> as well as Guy and Bhattacharya,<sup>14</sup> outline the methods of modeling cavity backed plates and investigate the dynamic effects. As with convected fluid loading, cavity backing can significantly affect the dynamics of the plate.

The effects of external fluid flow on the sound transmission have received only limited attention in the literature. Dowell<sup>15</sup> investigated a convected fluid loaded plate backed by a cavity emphasizing the effect on plate response. More recently, Koval<sup>16</sup> considered the sound transmission through a convected fluid loaded infinite plate into a half-space. Results from this investigation show slight decreases in sound transmission with increasing flow velocity. Finally, Clark and Frampton<sup>5</sup> considered sound transmission through a finite, aeroelastic plate into a half-space noting similar results.

Many recent efforts toward further understanding sound transmission through plates has focused on turbulent boundary-layer pressure transmission including structural and fluid nonlinearities.<sup>16,17</sup> These efforts noted that nonlinear effects can, in many situations, be important to accurately predict structural and fluid response.<sup>17</sup> Structural nonlinearities are important when the plate displacement is on the order of the plate thickness. Acoustic or fluid nonlinear effects become important when the pressure fluctuations are large compared to the ambient pressure. However, it was noted that, even when the plate motion is nonlinear in nature, the fluid response can be accurately predicted with linear acoustic theory.<sup>17</sup>

This investigation endeavors to develop a basic, linear physical model that can be readily analyzed to answer questions concerning effects of convected fluid loading on sound transmission and is practical for control system design investigations. The model combines the dynamic effects of an elastic plate subjected to fluid flow over one surface and coupled to an acoustic enclosure on the other surface.

Received July 19, 1996; revision received March 17, 1997; accepted for publication April 1, 1997. Copyright © 1997 by Kenneth D. Frampton and Robert L. Clark. Published by the American Institute of Aeronautics and Astronautics, Inc., with permission.

\*Research Assistant Professor, Department of Mechanical Engineering and Materials Science. Member AIAA.

†Assistant Professor, Department of Mechanical Engineering and Materials Science. Member AIAA.

This is based, in part, on the aeroelastic plate model developed by Frampton et al.<sup>18</sup> However, a singular value decomposition technique is employed for the aerodynamic modeling, as discussed by Frampton and Clark.<sup>19</sup> This aeroelastic plate model is then coupled to an acoustic cavity according to the method presented by Fahy.<sup>1</sup> Analytical results are presented that demonstrate the effects of variations in external flow speed on the sound transmitted to the cavity. Also, the importance of considering the cavity in the calculation of transmitted sound is discussed.

### Model Development

The model development begins with a discussion on modeling an elastic plate. This is followed by an overview of the aerodynamic forces on the plate due to the convected fluid loading. Next, the modeling of the cavity will be discussed along with coupling between the plate and cavity. Finally, a description of the model parameters used in this analysis will be presented.

#### Plate Dynamics

The aeroelastic plate in this investigation is modeled according to the method introduced by Frampton et al.<sup>18</sup> This method employs Galerkin's technique to discretize the linear equations of motion for the plate. The partial differential equation of motion describing a thin, uniform panel subjected to cavity pressures, convected fluid loading, and an independent disturbance pressure is<sup>20</sup>

$$D_s \nabla^4 w(x, y, t) + \rho_s h_s \frac{\partial^2 w(x, y, t)}{\partial t^2} = p^c(x, y, z = 0, t) - p^a(x, y, z = 0, t) - p^d(x, y, z = 0, t) \quad (1)$$

A separable solution is assumed using the in vacuo panel eigenfunctions and generalized coordinates of the form

$$w(x, y, t) = \sum_N \Psi_n(x, y) q_n(t) \quad (2)$$

where, for this investigation, the plate is assumed to be simply supported, thus having the following eigenfunctions:

$$\Psi_n(x, y) = \sin[(j\pi/a)x] \sin[(k\pi/b)y] \quad (3)$$

where the  $n$ th plate mode has indices  $(j, k)$ .

Substituting Eq. (2) into Eq. (1), multiplying by an arbitrary expansion function,  $\Psi_m(x, y)$ , and integrating over the domain yields a set of ordinary differential equations of the form

$$M_n [\ddot{q}_n(t) + \omega_n^2 q_n(t)] + \rho_a U_a^2 Q_n^a(t) + Q_n^d(t) + \rho_c S \sum_M C_{nm} \dot{\phi}_m^c(t) = 0 \quad (4)$$

where the coupling with the acoustic cavity, as expressed by the term

$$\rho_c S \sum_M C_{nm} \dot{\phi}_m^c(t)$$

is discussed later and the disturbance generalized forces are

$$Q_n^d(t) = \int_0^b \int_0^a p^d(x, y, z = 0, t) \Psi_n(x, y) dx dy \quad (5)$$

The aerodynamic generalized forces are defined by

$$Q_n^a(t) = \int_0^b \int_0^a \frac{p^a(x, y, z = 0, t)}{\rho_a U_a^2} \Psi_n(x, y) dx dy \quad (6)$$

and are described further in the following section.

#### External Flow Generalized Forces

The aerodynamic generalized forces  $Q_n^a(t)$  are found by solving the convected wave equation (or linearized potential flow equation)

$$\nabla^2 \Phi^a - \frac{1}{a^2} \left[ \frac{\partial^2 \Phi^a}{\partial t^2} + 2U_a \frac{\partial^2 \Phi^a}{\partial x \partial t} + U_a^2 \frac{\partial^2 \Phi^a}{\partial x^2} \right] = 0 \quad (7)$$

subject to the boundary conditions for a panel embedded in an infinite baffle:

$$\left. \frac{\partial \Phi^a}{\partial z} \right|_{z=0} = \begin{cases} \frac{\partial w}{\partial t} + U_a \frac{\partial w}{\partial x} & \text{on the panel} \\ 0 & \text{off the panel} \end{cases} \quad (8)$$

and a finiteness or radiation condition as  $z$  approaches infinity.

The solution can be obtained by taking a Laplace transform with respect to time and a double Fourier transform with respect to the  $x$  and  $y$  spatial coordinates.<sup>6</sup> The transformation is applied to Eqs. (7) and (8) and Bernoulli's equation

$$p^a = -\rho_a \left[ \frac{\partial \Phi^a}{\partial t} + U_a \frac{\partial \Phi^a}{\partial x} \right] \quad (9)$$

while incorporating Eq. (2). Details of the solution process can be found in Refs. 6 and 8.

The solution yields the generalized aerodynamic forces on the panel, which are given here as

$$Q_n^a(t) = \sum_N Q_{nn}^a \quad (10)$$

where

$$Q_{nn}^a(t) = q_n(t) S_{nn} + \dot{q}_n(t) D_{nn} + \int_0^t q_n(\tau) H_{nn}(t - \tau) d\tau + \int_0^t \dot{q}_n(\tau) I_{nn}(t - \tau) d\tau \quad (11)$$

The aerodynamic influence functions  $H_{nn}(t)$  and  $I_{nn}(t)$  are defined by integrals with no closed-form solution. Therefore, a singular value decomposition technique was used to approximate the aerodynamic system as presented by Frampton and Clark.<sup>19</sup> The resulting approximate aerodynamic system receives the plate generalized coordinates and their rates as inputs and provides the aerodynamic generalized forces on the plate as outputs. This aerodynamic model can then be coupled to the plate model as feedback resulting in a complete aeroelastic model.<sup>21, 22</sup>

#### Acoustic Cavity Dynamics

The equation of motion for the acoustic pressure in a cavity is

$$\nabla^2 p^c(x, y, z, t) - \frac{1}{a_c^2} \frac{\partial^2 p^c(x, y, z, t)}{\partial t^2} = \rho_c \frac{\partial^2 w(x, y, t)}{\partial t^2} \delta(z) \quad (12)$$

where  $\delta(z)$  is the spatial Dirac delta function. The forcing term in this equation results from assuming that the plate is a set of infinitesimal volume velocity sources in the  $z = 0$  plane.<sup>1</sup> Assuming the pressure is a series of the hard walled cavity eigenfunctions (corresponding to eigenvalues  $\alpha_m^c$ ) such that

$$p^c(x, y, z, t) = \sum_M \Gamma_m(x, y, z) a_m(t) \quad (13)$$

leads to the equation of motion for the cavity as outlined by Fahy<sup>1</sup>:

$$\Lambda_m \ddot{a}_m(t) + \Lambda_m (\alpha_m^c)^2 a_m(t) = \rho_c a_c^2 S \sum_N C_{nm} \ddot{q}_n(t) \quad (14)$$

where the modal volumes are expressed as

$$\Lambda_m = \int_V \Gamma_m^2(x, y, z) dV \quad (15)$$

and the coupling matrix for a plate having surface area  $S$  is

$$C_{nm} = \frac{1}{S} \int_S \Psi_n(x, y) \Gamma_m(x, y, z = 0) dS \quad (16)$$

When coupling the plate and cavity, however, it is more convenient to express the cavity dynamics in terms of the cavity fluid velocity potential  $\Phi^c(x, y, z, t)$ , which is related to the pressure as follows:

$$p^c(x, y, z, t) = -\rho_c \frac{\partial \Phi^c(x, y, z, t)}{\partial t} \quad (17)$$

The cavity velocity potential can be expressed as an expansion over the same set of functions as follows:

$$\Phi(x, y, z, t) = \sum_{m=1}^M \Gamma_m(x, y, z) \phi_m^c(t) \quad (18)$$

where  $\phi_m^c(t)$  is the generalized coordinate associated with the  $m$ th acoustic mode  $\Gamma_m(x, y, z)$ .

The equation of motion for the acoustic enclosure can then be expressed as

$$\Lambda_m \ddot{\phi}_m^c(t) + \Lambda_m (\alpha_m^c)^2 \phi_m^c(t) = a_c^2 S \sum_{n=1}^N C_{nm} \dot{q}_n(t) \quad (19)$$

### Model Parameters

The geometry of the investigated system is shown in Fig. 1, whereas physical dimensions of the system are shown in Table 1. Note that the plate occupies a portion of the cavity wall near one end of the cavity. The dimensions of the cavity were selected to be of a size approaching a small commercial aircraft cabin but limited to 50 acoustic modes in the same bandwidth as the first 20 plate modes. Proportional damping was also introduced into the plate and cavity equations by adding terms of the form  $2\zeta \omega_h \dot{q}_n$  and  $2\zeta \alpha_n^c \dot{\phi}_n^c$  into Eqs. (4) and (19), respectively.

The physical parameters of the system, including the plate, the external fluid, and the cavity, are listed in Table 2. The plate parameters correspond to those for aluminum whereas those for the external and internal fluids are typical values for an altitude of 10 km. These values were selected in order to simulate the typical structural and cruise conditions experienced by commercial aircraft previously detailed by Thomas and Nelson.<sup>23</sup>

**Table 1 System physical dimensions**

Variable	Description	Value, m
$L_x$	Cavity length	6.000
$L_y$	Cavity width	1.800
$L_z$	Cavity height	1.800
$a$	Plate length	0.600
$b$	Plate width	0.525
$x_p$	Plate coordinate	0.600
$y_p$	Plate coordinate	0.600

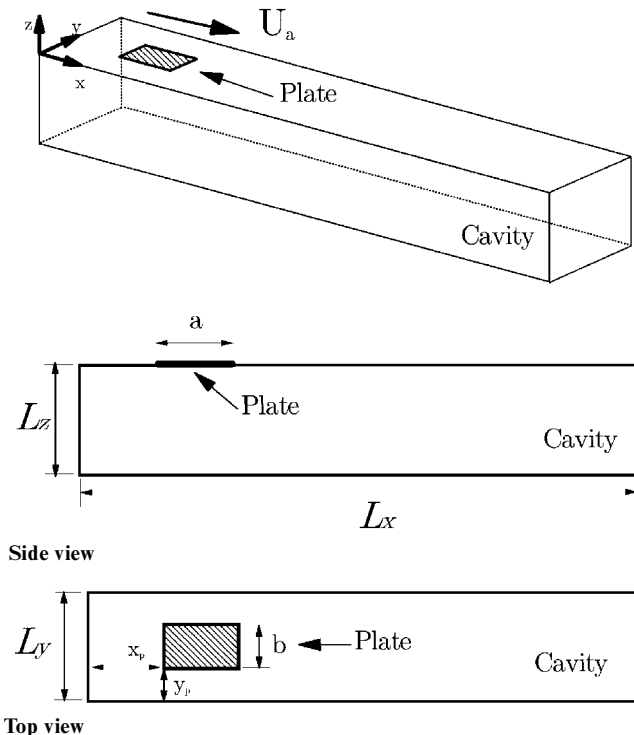


**Fig. 1 System schematic.**

**Table 2 System parameters**

Variable	Description	Value
<i>Plate parameters</i>		
$E_s$	Modulus	$7.1 \times 10^{10}$ N/m <sup>2</sup>
$\rho_s$	Density	2700 kg/m <sup>3</sup>
$h_s$	Thickness	0.0022 m
$\nu_s$	Poisson's ratio	0.3
$\zeta$	Damping ratio	0.01
$N$	Modes	20
<i>Cavity fluid parameters</i>		
$\rho_c$	Fluid density	0.42 kg/m <sup>3</sup>
$a_c$	Speed of sound	310 m/s
$\zeta$	Damping ratio	0.05
$M$	Modes	50
<i>External fluid parameters</i>		
$\rho_a$	Fluid density	0.42 kg/m <sup>3</sup>
$a_a$	Speed of sound	310 m/s
$U_a$	Flow velocity	31–620 m/s

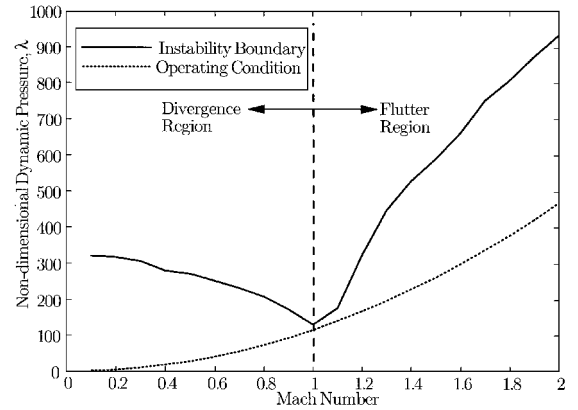


**Fig. 2 Comparison of system operating condition to the system stability boundary.**

The basic model was constructed as outlined earlier with 20 plate modes and 50 cavity modes. The highest plate and cavity modes had frequencies near 550 Hz; however, results are presented for 0–300 Hz only, which includes the first 10 plate modes and the first 30 cavity modes. The inclusion of modes beyond the frequency range of interest ensured that the lower model modes had converged.<sup>24</sup>

The external aerodynamic model for this investigation was computed for the first 10 plate modes. This was deemed sufficient when the results for the four-mode aeroelastic plate of Refs. 18 and 22 were compared to the model used here. Because the cavity acoustic response is dominated by the lowest acoustic modes the addition of more aeroelastic coupled modes does not significantly alter the system response. Sufficient accuracy was achieved with 55 states for the subsonic aerodynamic systems and 60 states for the supersonic systems.<sup>19</sup>

An important consideration involving the system parameters is how close the system operates to the flutter or divergence boundary at each operating point. The flutter dynamic pressure vs Mach number is shown in Fig. 2 along with the system operating condition. The external flow velocity was varied between 31 and 620 m/s corresponding to a variation in Mach number between 0.1 and 2.0. Note that the system is below the flutter/divergence curve for all Mach numbers. Also notice that the system comes very close to the instability margin near  $M = 1.0$  and  $1.1$ . This fact will be important in later descriptions of the system behavior.

### Results

The primary focus of this investigation is to study how changes in external flow affect the transmission of sound into the acoustic cavity. This will be quantified in terms of the cavity acoustic potential energy

$$E^c = \frac{1}{2\rho_c a_c^2} \int_V [p^c(x, y, z, t)]^2 dV \quad (20)$$

If the time average of this equation is considered, along with power spectral and transfer function relations, the acoustic power spectral density can be expressed in terms of the cavity velocity potential as

$$\mathcal{P}(\omega) = \frac{\rho_c}{2a_c^2} \sum_{m=1}^M \sum_{n=1}^N \Lambda_m |H_{\phi_m Q_n}(\omega)|^2 \mathcal{P}_{Q_n}^d(\omega) \quad (21)$$

where  $H_{\phi_m Q_n}(\omega)$  is the transfer function between the  $n$ th generalized disturbance force and the  $m$ th cavity velocity potential generalized coordinate.  $\Lambda_m$  is the result of Eq. (15).

The disturbance considered in this investigation consists of equal, constant amplitude power spectra for each generalized force, i.e.,  $\mathcal{P}_{Q_n}^d(\omega) = 2.132 \times 10^{-4} \text{ N}^2\text{s}$  for all inputs. Certainly this represents an oversimplified and nonrealistic disturbance; however, it removes the effects of a varying system disturbance allowing the effects of varying external flow to be studied in an independent manner. The implications of a more typical turbulent boundary-layer disturbance, which scales with the Mach number squared, will be discussed.

The first comparison, shown in Figs. 3 and 4, displays the cavity potential energy spectrum at various subsonic and supersonic Mach numbers, respectively. As illustrated, the cavity energy is dominated by the coupled system resonance at about 35 Hz. Recall that the model is fully coupled so that the system modes are a combination of all in vacuo modes including those of the cavity, plate, and aerodynamics. However, it is insightful to relate these coupled modes to the in vacuo modes. In this light, the dominant mode of the coupled system occurs at a frequency very near the first plate mode. Note in Fig. 3 that, as the flow velocity approaches  $M = 1.0$ , the frequency of the fundamental plate mode decreases. This is due to the plate closely approaching the divergence flow velocity. Divergence is a

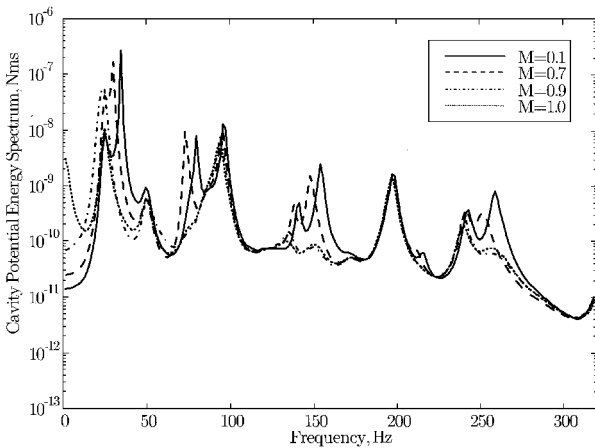


Fig. 3 Cavity potential energy power spectra at various subsonic Mach numbers.

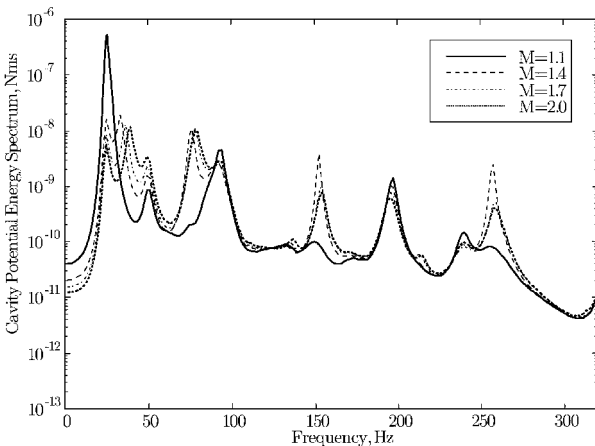


Fig. 4 Cavity potential energy power spectra at various supersonic Mach numbers.

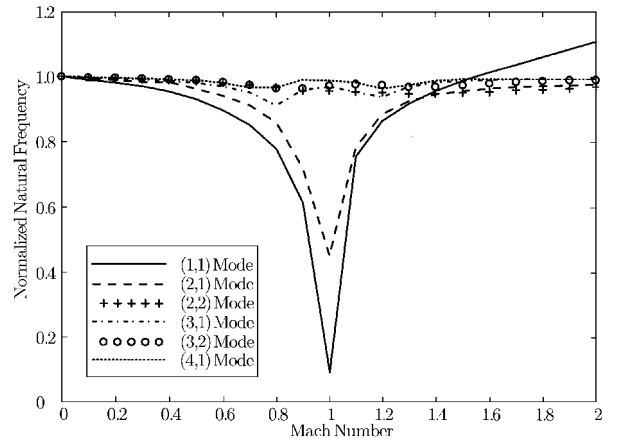


Fig. 5 Coupled system normalized natural frequencies vs Mach number.

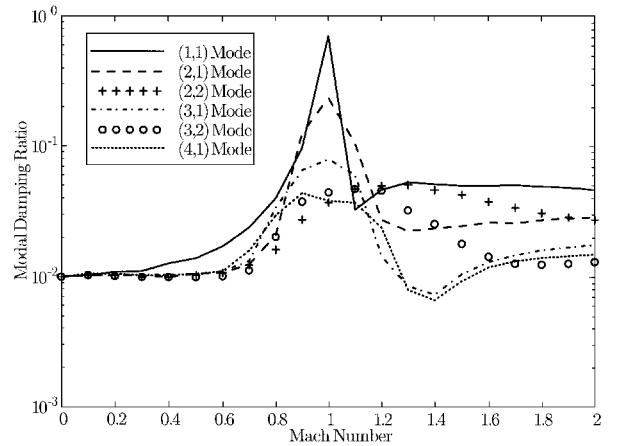


Fig. 6 Coupled system modal damping ratios vs Mach number.

zero frequency (or static) instability created by coupling with the external flow.<sup>8</sup>

This effect is more apparent in Fig. 5, which shows the natural frequencies of the first six plate modes normalized with respect to the in vacuo plate natural frequencies as a function of Mach number. Even at higher Mach numbers, these coupled modes are dominated by the respective in vacuo plate modes and are designated as such in the figure. Note that the greatest effect is on the fundamental plate mode. For this combination of system parameters, the fundamental plate mode natural frequency is reduced by a factor of 10 at  $M = 1.0$ . The (2, 1) mode is also significantly affected whereas all other modes change by less than 10%.

The external flow affects not only the system natural frequencies but also the modal damping. The damping ratios of the first six (coupled) plate modes as a function of Mach number are shown in Fig. 6. As with natural frequency, the fundamental plate mode experiences the greatest effect, particularly near  $M = 1.0$ . This effect has previously been called aerodynamic damping or radiation damping and is due to the loss of energy to the external fluid as acoustic radiation.<sup>25</sup> The combined effect of modified natural frequency and damping ratio indicates that the external flow serves to modify the plate impedance, which is expected to have an effect on sound transmission. This change in the plate impedance would be particularly important when designing an active control system. Any control system designed without these effects would certainly perform nonoptimally in the presence of flow, and the robustness of the control system would also suffer.

The total acoustic potential energy as a function of Mach number is shown in Fig. 7. Note that the cavity energy generally decreases with increasing flow speed. However, a large decrease is seen as the flow approaches  $M = 1.0$ , followed by a sharp increase near  $M = 1.1$ . The cavity energy trend near  $M = 1.0$  is dictated by the

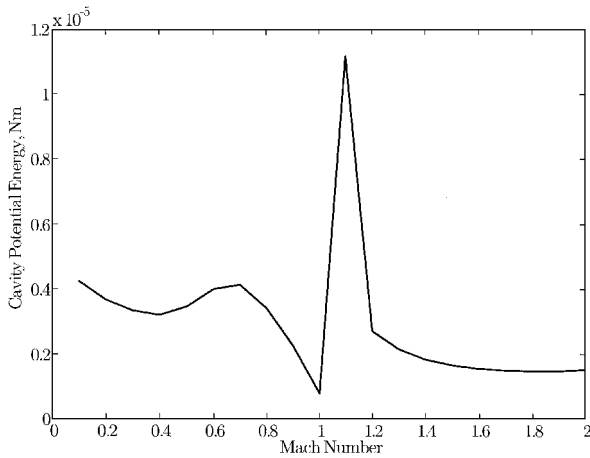


Fig. 7 Total cavity potential energy vs Mach number.

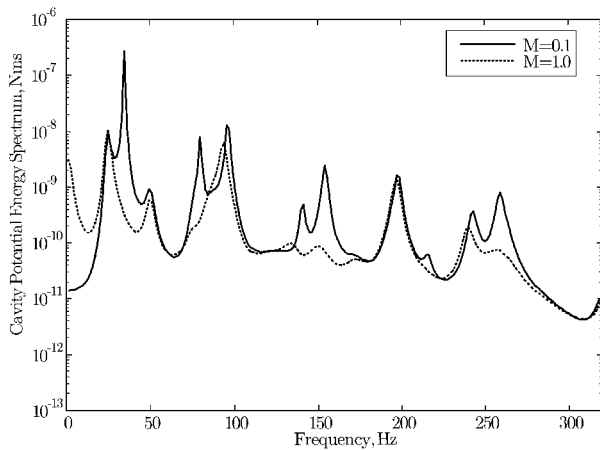


Fig. 8 Cavity potential energy power spectra at  $M = 0.1$  and  $1.0$ .

aerodynamic damping experienced by the plate, as shown in Fig. 6. The curve in Fig. 7 depicting cavity potential energy is approximately inversely proportional to the (1, 1) mode damping curve of Fig. 6 (excepting the region near  $M = 1.1$ ). Also note that the variation in cavity acoustic energy is within a single order of magnitude. This is consistent with previously published results.<sup>3,5</sup>

An important consideration is to determine whether the inclusion of coupling with the acoustic cavity is important to accurately calculate the transmitted noise levels. Consider Fig. 8, which shows the cavity potential energy power spectra for Mach numbers of 0.1 and 1.0. Note that the cavity potential energy at  $M = 0.1$  is dominated by the spectral peaks at 35, 80, and 97 Hz, which are associated with the (1, 1), (2, 1), and (1, 2) plate modes. The two peaks which straddle the fundamental plate mode peak (near 25 and 50 Hz) are associated with the first two cavity modes. In this situation, which corresponds to light aerodynamic coupling, the total cavity potential energy could be accurately represented without considering the cavity coupling. However, when the aerodynamic coupling becomes strong near  $M = 1.0$ , the situation changes. Near  $M = 1.0$ , the aerodynamic coupling has a large effect on the frequency and damping of the (1, 1) and (2, 1) plate modes, as demonstrated in Figs. 5 and 6. In this situation, the cavity potential energy is dominated by the first cavity mode (near 25 Hz), as shown in Fig. 8. The (1, 2) plate mode also has a significant effect inasmuch as it is affected very little by the aerodynamic loading. Therefore, inclusion of the cavity model is important when the aerodynamic effects become large.

Furthermore, in the supersonic flow regime the fundamental plate mode experiences significant changes in natural frequency while simultaneously having relatively low damping. At some point, while the fundamental plate mode migrates in frequency, it comes into coincidence with one of the acoustic modes, resulting in strong coupling between the plate and cavity. This occurs for this system

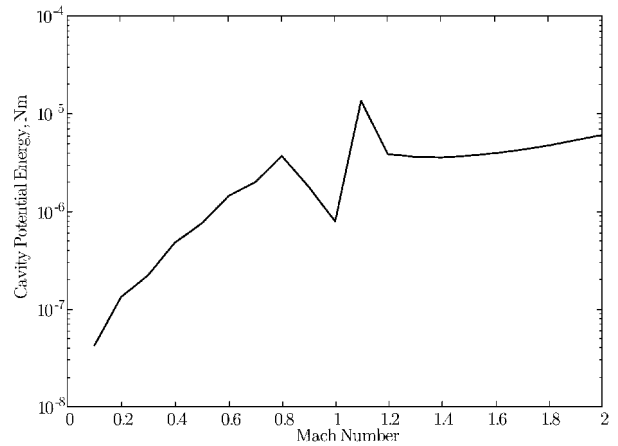


Fig. 9 Total cavity potential energy vs Mach number for a scaled disturbance.

configuration at  $M = 1.1$  and is demonstrated by the exaggerated spectral peak at 25 Hz in Fig. 4 causing the dramatic increase in transmitted energy at  $M = 1.1$  shown in Fig. 7. This further demonstrates the importance of including the cavity model when calculating the transmitted sound through an aeroelastic plate.

Note that the results in Fig. 6 are for a disturbance that remains constant with Mach number. A more realistic turbulent boundary-layer pressure disturbance, however, is known to scale approximately with the Mach number squared.<sup>26</sup> For illustrative purposes, the system disturbance was varied with flow velocity squared such that  $\mathcal{P}_{p, Q^d}(\omega) = (\frac{1}{2}\rho_a U_a^2)^2 5.235 \times 10^{-13} \text{ N}^2\text{s}$  for each generalized force power spectra. Although this still does not capture the true nature of turbulent boundary-layer pressures, it does illustrate the effect that a realistic, scaled disturbance has on the total cavity potential energy. This is demonstrated in Fig. 9. A comparison between the cavity energy trend for a constant disturbance (Fig. 7) and the scaled disturbance trend (Fig. 9) indicates that the scaling of the turbulent boundary-layer pressure amplitude greatly outweighs the aerodynamic damping effects. As the Mach number increases from 0.1 to 2.0, an increase of several orders of magnitude is noted in Fig. 9, which is consistent with previous results.<sup>5</sup>

## Conclusions

A method for modeling sound transmission through an aeroelastic plate into a cavity has been presented. The primary purpose was to investigate the effects of variations in external flow velocity on the sound transmission. It was noted that increases in external flow generally decrease the transmission of a constant amplitude disturbance. The cause of this decrease was shown to be modification of the plate impedance due to an increase in the aerodynamic damping. However, in supersonic flow conditions, the migration of the fundamental aeroelastic plate mode will create a coincidence with a cavity mode resulting in exceptional coupling and increases in the transmitted sound. When a more realistic turbulent boundary-layer disturbance is considered, which scales with the Mach number squared, the overall effect is an increase in the transmitted sound by several orders of magnitude with increasing Mach number. It was also noted that when the aerodynamic effects were prevalent, i.e., high subsonic and supersonic flow, inclusion of the cavity coupling is important for accurately predicting the transmitted sound.

## Acknowledgments

The authors would like to acknowledge the support of National Science Foundation (NSF) Graduate Traineeship EE-92-56573 and NSF Career Program CMS-9501470.

## References

- Fahy, F., *Sound and Structural Vibration*, Academic, London, 1985, Chap. 6.
- Crighton, D. G., "The 1988 Rayleigh Medal Lecture: Fluid Loading—The Interaction Between Sound and Vibration," *Journal of Sound and Vibration*, Vol. 133, No. 1, 1989, pp. 1–27.

- <sup>3</sup>Koval, L. R., "Effect of Air Flow, Panel Curvature, and Internal Pressurization on Field-Incidence Transmission Loss," *Journal of the Acoustical Society of America*, Vol. 59, No. 6, 1976, pp. 1379–1385.
- <sup>4</sup>Atalla, N., and Nicolas, J., "A Formulation for Mean Flow Effects on Sound Radiation from Rectangular Baffled Plates with Arbitrary Boundary Conditions," *Journal of Vibration and Acoustics*, Vol. 117, No. 1, 1995, pp. 22–29.
- <sup>5</sup>Clark, R. L., and Frampton, K. D., "Aeroelastic Structural Acoustic Coupling: Implications on the Control of Turbulent Boundary Layer Noise Transmission," *Journal of the Acoustical Society of America* (to be published).
- <sup>6</sup>Dowell, E. H., "Generalized Aerodynamic Forces on a Flexible Plate Undergoing Transient Motion," *Quarterly of Applied Mathematics*, Vol. 26, No. 3, 1967, pp. 2267–2270.
- <sup>7</sup>Dowell, E. H., "Panel Flutter: A Review of the Aeroelastic Stability of Plates and Shells," *AIAA Journal*, Vol. 8, No. 3, 1970, pp. 385–399.
- <sup>8</sup>Dowell, E. H., *Aeroelasticity of Plates and Shells*, Noordhoff International, Leyden, The Netherlands, 1975, Chap. 4.
- <sup>9</sup>Dugundji, J., "Theoretical Considerations of Panel Flutter at High Supersonic Mach Numbers," *AIAA Journal*, Vol. 4, No. 7, 1966, pp. 1257–1266.
- <sup>10</sup>Hedgepeth, J. M., "Flutter of Rectangular Simply Supported Panels at High Supersonic Speeds," *Journal of the Aeronautical Sciences*, Vol. 24, No. 8, 1957, pp. 563–573.
- <sup>11</sup>Dowell, E. H., and Voss, H. M., "The Effect of a Cavity on Panel Vibration," *AIAA Journal*, Vol. 1, No. 2, 1962, pp. 476–477.
- <sup>12</sup>Fahy, F. J., "Vibration of Containing Structures by Sound in the Contained Fluid," *Journal of Sound and Vibration*, Vol. 10, No. 3, 1969, pp. 490–512.
- <sup>13</sup>Pretlove, A. J., "Forced Vibrations of a Rectangular Panel Backed by a Closed Rectangular Cavity," *Journal of Sound and Vibrations*, Vol. 3, No. 3, 1966, pp. 252–261.
- <sup>14</sup>Guy, R. W., and Bhattacharya, M. C., "The Transmission of Sound Through a Cavity-Backed Finite Plate," *Journal of Sound and Vibration*, Vol. 27, No. 2, 1973, pp. 207–223.
- <sup>15</sup>Dowell, E. H., "Transmission of Noise from a Turbulent Boundary Layer Through a Flexible Plate into a Closed Cavity," *Journal of the Acoustical Society of America*, Vol. 46, No. 1, 1969, pp. 238–252.
- <sup>16</sup>Wu, S. F., and Maestrello, L., "Responses of Finite Baffled Plate to Turbulent Flow Excitations," *AIAA Journal*, Vol. 33, No. 1, 1995, pp. 13–19.
- <sup>17</sup>Frendi, A., Maestrello, L., and Ting, L., "An Efficient Model for Coupling Structural Vibration with Acoustic Radiation," *Journal of Sound and Vibration*, Vol. 182, No. 5, 1995, pp. 741–757.
- <sup>18</sup>Frampton, K. D., Clark, R. L., and Dowell, E. H., "State Space Modeling for Aeroelastic Panels Subject to Full Potential Flow Aerodynamic Loading," *Proceedings of the AIAA 36th Structures, Structural Dynamics, and Materials Conference* (New Orleans, LA), AIAA, Washington, DC, 1995, pp. 1183–1189.
- <sup>19</sup>Frampton, K. D., and Clark, R. L., "State Space Modeling of Aerodynamic Forces on a Plate Using Singular Value Decomposition," *AIAA Journal*, Vol. 34, No. 12, 1996, pp. 2627–2630.
- <sup>20</sup>Meirovitch, L., *Analytical Methods in Vibrations*, Macmillan, New York, 1967, Chap. 5.
- <sup>21</sup>Frampton, K. D., and Clark, R. L., "Power Flow in an Aeroelastic Plate Backed by a Reverberant Cavity," *Journal of the Acoustical Society of America* (submitted for publication).
- <sup>22</sup>Frampton, K. D., Clark, R. L., and Dowell, E. H., "State Space Modeling for Aeroelastic Panels Subject to Full Potential Flow Aerodynamic Loading," *Journal of Aircraft*, Vol. 33, No. 4, 1996, pp. 816–822.
- <sup>23</sup>Thomas, D. R., and Nelson, P. A., "Feedback Control of Sound Radiation from a Plate Excited by a Turbulent Boundary Layer," *Journal of the Acoustical Society of America*, Vol. 98, No. 5, 1995, pp. 2651–2662.
- <sup>24</sup>Clark, R. L., "Accounting for Out-of-Bandwidth Modes in the Assumed Modes Approach: Implications on Colocated Output Feedback Control," *Journal of Dynamic Systems, Measurement and Control* (to be published).
- <sup>25</sup>Lyle, K. H., and Dowell, E. H., "Acoustic Radiation Damping of Flat Rectangular Plates Subjected to Subsonic Flows, Parts I and II," *Journal of Fluids and Structures*, Vol. 8, No. 7, 1994, pp. 711–746.
- <sup>26</sup>Blake, W. K., "Turbulent Boundary-Layer Wall-Pressure Fluctuations on Smooth and Rough Walls," *Journal of Fluid Mechanics*, Vol. 44, No. 4, 1970, pp. 637–660.

S. Glegg  
Associate Editor